

# Cross-RAG: Zero-Shot Retrieval-Augmented Time Series Forecasting via Cross-Attention

Seunghan Lee<sup>1</sup> Jaehoon Lee<sup>1</sup> Jun Seo<sup>1</sup> Sungdong Yoo<sup>1</sup> Minjae Kim<sup>1</sup>  
Tae Yoon Lim<sup>1</sup> Dongwan Kang<sup>1</sup> Hwanil Choi<sup>1</sup> SoonYoung Lee<sup>1</sup> Wonbin Ahn<sup>1</sup>

## Abstract

Recent advances in time series foundation models (TSFMs) demonstrate strong expressive capacity through large-scale pretraining across diverse time series domains. Zero-shot time series forecasting with TSFMs, however, exhibits limited generalization to unseen datasets, which retrieval-augmented forecasting addresses by leveraging an external knowledge base. Existing approaches rely on a fixed number of retrieved samples that may introduce *irrelevant* information. To this end, we propose **Cross-RAG**, a zero-shot retrieval-augmented forecasting framework that selectively attends to query-relevant retrieved samples. Cross-RAG models input-level relevance between the query and retrieved samples via *query–retrieval cross-attention*, while jointly incorporating information from each of the query and retrieved samples. Extensive experiments demonstrate that Cross-RAG consistently improves zero-shot forecasting performance across various TSFMs and RAG methods, with additional analyses confirming its effectiveness across various retrieval scenarios. Code is available at: <https://github.com/seunghan96/cross-rag/>.

## 1 Introduction

Time series (TS) forecasting is widely adopted across diverse domains, including finance (Rezaei et al., 2021) and traffic systems (Cirstea et al., 2022). Deep learning–based approaches, such as recurrent (Xu et al., 2025), convolutional (Luo & Wang, 2024), graph-based (Huang et al., 2023), and transformer-based models (Liu et al., 2024b), effectively capture temporal dependencies, while their training remains largely confined to domain-specific datasets.

Recent studies investigate time series foundation models (TSFMs) to enable more generalizable forecasting through

<sup>1</sup>LG AI Research, Seoul, South Korea. Correspondence to: Wonbin Ahn <wonbin.ahn@lgresearch.ai>.

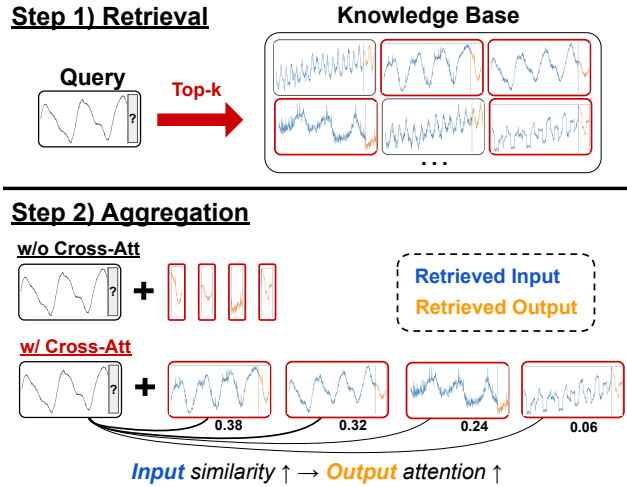


Figure 1. **Cross-attention btw query & retrieved inputs.** While previous works aggregate retrieved samples without explicitly modeling the relationship between the query and the retrieved inputs, Cross-RAG performs *input-aware* fusion by using *cross-attention* to weight retrieved samples based on the input similarity.

large-scale pretraining (Jiang et al., 2025; Tan et al., 2024; Ansari et al., 2024; Das et al., 2024). Despite their expressive capacity, these models exhibit limited robustness in zero-shot settings due to distribution mismatch between the pretraining and unseen datasets, incur substantial adaptation cost, and lack mechanisms for dynamic domain conditioning and interpretability (Ning et al., 2025).

Recently, retrieval-augmented generation (RAG) enhances context awareness across diverse tasks by retrieving relevant contextual evidence and incorporating it into model inputs. Several studies extend this paradigm to TS forecasting (Ning et al., 2025; Han et al., 2025; Yang et al., 2025), seeking to leverage historical patterns through retrieval mechanisms. However, existing RAG-based approaches for TS forecasting either rely on dataset-specific adaptation rather than zero-shot inference or fail to fully exploit the input structure of retrieved samples during forecasting.

To this end, we propose **Cross-RAG**, a zero-shot retrieval-augmented forecasting framework which models input-level relevance between the query and retrieved samples by attending to their inputs via (query–retrieval) *cross-attention*, as illustrated in Figure 1. Specifically, the prediction in-

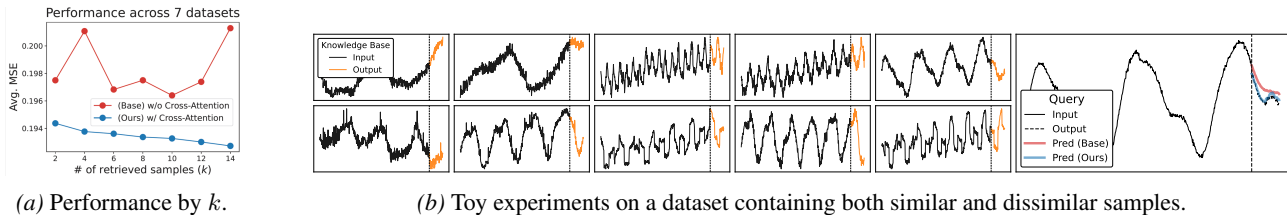


Figure 2. **Experiments w/ and w/o cross-attention.** (a) The figure shows that, with cross-attention, performance improves as the number of retrieved samples ( $k$ ) increases. (b) The figure presents zero-shot forecasting results on toy datasets with 10 retrieved samples ( $k = 10$ ) for both methods, with and without cross-attention (Ning et al., 2025), where our method accurately matches the ground truth.

Table 1. **Comparison of TS RAG frameworks.** (1) *How to retrieve?* Defines the similarity space used for retrieval in either the data space or the latent space, depending on the use of the retrieval encoder  $h(\cdot)$ . (2) *What to retrieve?* Specifies the retrieved content  $R$ . (3) *How to fuse?* Describes how the retrieved information is integrated with the query  $Q$ .

Method		1. How to retrieve?	2. What to retrieve?	3. How to fuse?
Full-shot	RAFT (ICML 2025)	$Q$ vs. $R_x$	$R_y$	Concatenate
	RATD (NeurIPS 2024)	$Q$ vs. $h(R_x)$	$(R_x, R_y)$	Cross-Attention <sup>(1)</sup>
	TimeRAG (ICASSP 2025)	$Q$ vs. $R_x$	$R_x$	$\chi$ <sup>(2)</sup>
Zero-shot	RAF (arXiv 2025)	$Q$ vs. $h(R_x)$	$(R_x, R_y)$	$\chi$ <sup>(3)</sup>
	TS-RAG (NeurIPS 2025)	$Q$ vs. $h(R_x)$	$R_y$	Self-Attention
	Cross-RAG (Ours)	$Q$ vs. $R_x$	$(R_x, R_y)$	Cross-Attention

<sup>(1)</sup> The cross-attention mechanism in **RATD** is fundamentally different from ours, as it attends over retrieved samples using both  $(R_x, R_y)$  as keys and dataset-level auxiliary statistics as values, rather than modeling query–retrieval interactions at the input level.

<sup>(2)</sup> **TimeRAG** converts retrieved input sequences into text prompts and feeds them into an LLM backbone.

<sup>(3)</sup> **RAF** forms a single long sequence by prepending retrieved samples to the query without modeling interaction between them.

tegrates three sources of information: 1) the query itself, 2) the retrieved samples themselves, and 3) the relational information between the query and retrieved samples.

As shown in Figure 2a, Cross-RAG consistently improves performance (average MSE across seven datasets) as the number of retrieved samples ( $k$ ) increases by selectively leveraging relevant samples even when irrelevant ones may be included. Figure 2b shows that methods without cross-attention (Ning et al., 2025) fail on a toy dataset where irrelevant samples are retrieved, while Cross-RAG succeeds.

The main contributions are summarized as follows:

- We propose **Cross-RAG**, a plug-in framework that enhances retrieval-augmented forecasting by *selectively* attending to retrieved samples according to their relevance to the query, using *cross-attention* between the query and the inputs of the retrieved samples.
- To the best of our knowledge, Cross-RAG is the first zero-shot RAG approach to model relationships between the query and retrieved inputs, as shown in Table 1.
- We validate Cross-RAG through extensive experiments, achieving state-of-the-art (SoTA) performance across diverse datasets. The proposed method supports zero-shot forecasting, enabling efficient integration without requiring additional retraining of target datasets.
- We conduct in-depth analyses under various retrieval conditions, demonstrating its ability to selectively attend to relevant samples while remaining robust to the inclusion of irrelevant retrieved samples.

## 2 Related Works

**Time series foundation models (TSFMs).** TSFMs have emerged as a scalable alternative to LLM-based forecasters, which incur high computational costs and domain adaptation challenges (Zhou et al., 2023; Xue & Salim, 2023; Chang et al., 2023; Sun et al., 2024; Niu et al., 2025). Early works introduce large-scale pretraining for TS forecasting (Rasul et al., 2023; Garza et al., 2023), followed by Transformer-based extensions (Liu et al., 2024c; 2025). Recent models commonly adopt patch-based tokenization to embed continuous TS, where TimesFM (Das et al., 2024) and MOMENT (Goswami et al., 2024) model patch-level representations to enable forecasting across diverse datasets, while TTM (Ekambaram et al., 2024) improves efficiency through compact architectures with reduced parameterization. TimeMoE (Shi et al., 2025) further enhances scalability by adopting a sparse mixture-of-experts design. Beyond deterministic forecasting, Moirai (Woo et al., 2024) learns mixtures of predictive distributions to capture uncertainty. Chronos (Ansari et al., 2024) formulates forecasting as a language modeling task by discretizing scaled TS into categorical tokens, and Chronos-Bolt replaces discrete tokenization with patch-based inputs and produces multi-step quantile forecasts. Despite strong generalization, these models rely on internal representations and lack mechanisms to dynamically incorporate external knowledge, which limits interpretability and zero-shot adaptability (Ning et al., 2025).

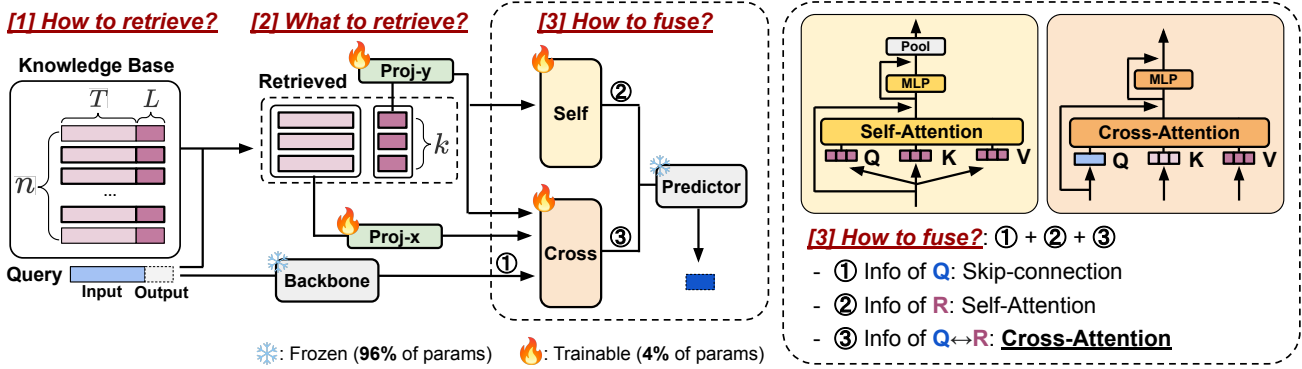


Figure 3. **Overall Framework of Cross-RAG.** Cross-RAG fuses retrieved information through two branches: (1) *Query–retrieval cross-attention* models relevance between the query and retrieved inputs and aggregates retrieved outputs conditioned on this relevance. (2) *Retrieval self-attention* summarizes retrieved outputs in a query-independent manner to capture contextual information among retrieved samples. The TSFM backbone and predictor are frozen, and only the additional modules are trained on general pretraining datasets.

### Retrieval-augmented generation (RAG) in time series.

RAG (Lewis et al., 2020) provides a principled way to incorporate external knowledge and improve robustness, and recent studies extend this paradigm to TS forecasting. ReTime (Jing et al., 2022) introduces relational retrieval with content synthesis, RATD (Liu et al., 2024a) leverages retrieved historical series to guide diffusion-based denoising, and RAFT (Han et al., 2025) combines retrieval with multi-resolution forecasting. TimeRAG (Yang et al., 2025) incorporates retrieved sequences through a frozen LLM backbone with a trainable reprogramming layer to align modalities. However, these approaches are limited in that they *require fine-tuning on the target set* for adaptation to unseen datasets.

Recently, zero-shot<sup>1</sup> RAG methods have also been introduced for TS forecasting. RAF (Tire et al., 2024) constructs an augmented input by concatenating retrieved sequences with the query sequence in the raw data space. TS-RAG (Ning et al., 2025) retrieves TS segments using a pretrained encoder and integrates them into the forecasting process by conducting self-attention with concatenated query and retrieved outputs. However, these approaches *do not explicitly account for the relationship between the query and the retrieved inputs* when aggregating the retrieved samples. Comparison of RAG methods in TS is shown in Table 1.

## 3 Methodology

**TS forecasting with RAG.** We consider the task of TS forecasting with retrieval augmentation. Let  $\mathcal{D} = \{(\mathbf{x}_j, \mathbf{y}_j)\}_{j=1}^n$  denote a retrieval knowledge base, where  $\mathbf{x}_j \in \mathbb{R}^T$  is an input window of length  $T$  and  $\mathbf{y}_j \in \mathbb{R}^L$  is the corresponding forecasting horizon of length  $L$ . Given a query input  $\mathbf{x}_i$ , our goal is to predict  $\hat{\mathbf{y}}_i$  by leveraging both the query input and a set of retrieved samples from  $\mathcal{D}$ .

<sup>1</sup>Zero-shot in RAG refers to settings where no data from the *target task dataset* is used for parameter updates, and models are pretrained solely on large-scale, *task-independent TS corpora*.

Table 2. **1) How to retrieve?** Robustness to choice of similarity space and retrieval metric (Average MSE across 7 datasets).

Retrieval space & Metric		Retrieval encoder	Avg. MSE
Data	Cosine		0.191
	Euclidean	✗	0.193
	Correlation		0.194
Latent		✓	0.193

In this section, we organize our retrieval-augmented forecasting framework into three key aspects:

- Section 3.1 (**How to Retrieve**) covers the choice of similarity space and metric for selecting relevant samples.
- Section 3.2 (**What to Retrieve**) specifies which parts of the retrieved samples—inputs, outputs, or both—are used.
- Section 3.3 (**How to Fuse**) describes how query and retrieved information are aggregated to produce a final representation for forecasting.

The overall framework of our method is shown in Figure 3.

### 3.1 How to Retrieve

A key design choice in RAG for TS forecasting is the retrieval space, where we analyze retrieval performed in the *data space* and the *latent space*. Table 2 reports the average MSE across seven datasets using four different similarity metrics, showing that our method remains robust across retrieval spaces and metrics. This result contrasts with prior studies (Ning et al., 2025; Liu et al., 2024a), which report inferior performance with data-space retrieval. In contrast, our method achieves comparable performance in both spaces, while data-space retrieval avoids the need for an additional retrieval encoder (i.e., a *retriever*) and thus offers a more efficient alternative, which is further discussed in Section 5.3.

Based on this observation, we adopt data-space retrieval in our framework. Formally, given a cosine similarity on the input space, we retrieve the top- $k$  most similar samples to  $\mathbf{x}_i$  from the dataset  $\mathcal{D}$ , denoted as  $\mathcal{R}_i$ .

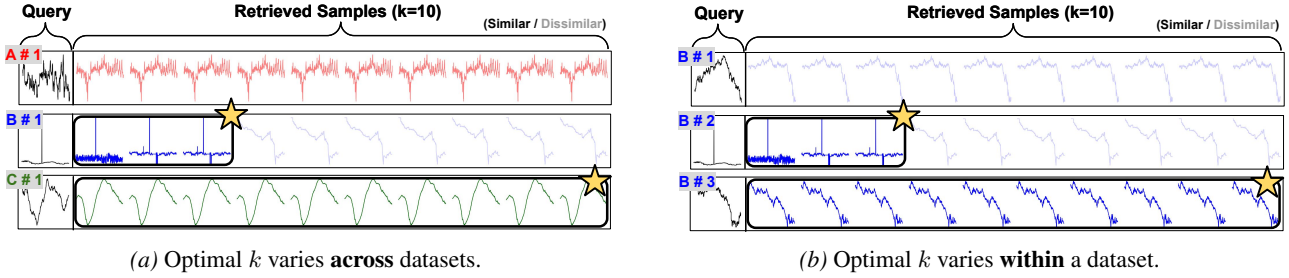


Figure 4. **Necessity of selective attention.** The figure shows that the optimal  $k$  varies both *across* and *within* datasets ([A] ETTh1, [B] Exchange, [C] Weather), highlighting the necessity of selectively attending to samples among the retrieved samples.

### 3.2 What to Retrieve

Selecting a fixed top- $k$  retrieved samples can be problematic, as the optimal  $k$  depends on how many samples in the knowledge base are similar to the query, and a fixed  $k$  may include *irrelevant ones* when this number varies. Figure 2b illustrates this issue on toy datasets with both similar and dissimilar samples, where the previous method (Ning et al., 2025) fail to accurately capture the ground truth.

As shown in Figure 4a, the optimal  $k$  differs *across* datasets. Moreover, Figure 4b shows that even *within* the same dataset, the number of samples similar to a given query varies across queries, highlighting the necessity to *selectively attend to relevant samples* among the retrieved ones.

To address this issue, we fuse information between the query and the retrieved samples by explicitly modeling the relationship between the query and the retrieved inputs. Each retrieved element in  $\mathcal{R}_i$  is represented as an input–output pair  $(x_j, y_j)$ , which are mapped into  $d$ -dimensional latent spaces via MLP-based projectors. Formally, we compute

$$r_{x,j} = f_x(x_j), \quad r_{y,j} = f_y(y_j) \quad (1)$$

for each retrieved pair  $(x_j, y_j) \in \mathcal{R}_i$ , where  $f_x(\cdot)$  and  $f_y(\cdot)$  denote the input and output projectors, respectively.

### 3.3 How to Fuse

Given a query  $x$  and its retrieved set  $\mathcal{R} = \{(r_{x,j}, r_{y,j})\}_{j=1}^k$ , we integrate query and retrieved information by explicitly modeling their input-level relevance<sup>2</sup>. Let  $h \in \mathbb{R}^d$  denote the query representation produced by an arbitrary TSFM backbone, and let  $R_x \in \mathbb{R}^{k \times d}$  and  $R_y \in \mathbb{R}^{k \times d}$  denote the stacked representations of retrieved inputs and outputs.

**Query–Retrieval Cross-Attention.** The proposed method applies cross-attention to selectively incorporate retrieval information relevant to the query, using the query representation as the *query* and the retrieved inputs and outputs as the *keys* and *values* of attention-mechanism, respectively:

$$c = \text{Attn}(h, R_x, R_y) + h. \quad (2)$$

<sup>2</sup>For simplicity, we omit the query index in this section.

Here,  $\text{Attn}(\cdot)$  denotes a multi-head attention block, and the residual connection preserves the information of the query itself. The attended representation is further processed by a feed-forward network with a residual connection:

$$\tilde{c} = \text{FFN}_{\text{cross}}(c) + c. \quad (3)$$

This operation selectively extracts information from the retrieved outputs by weighting them according to the relevance of their corresponding inputs to the query.

**Retrieval Self-Attention.** To summarize the retrieved samples independently of the query, Cross-RAG applies self-attention over their outputs:

$$s = \text{Attn}(R_y, R_y, R_y) + R_y, \quad (4)$$

followed by a feed-forward network and aggregation:

$$\tilde{s} = \text{Pool}(\text{FFN}_{\text{self}}(s) + s), \quad (5)$$

where  $\text{Pool}(\cdot)$  denotes mean pooling over the retrieved samples. This operation captures retrieval-driven information by aggregating the outputs of the top- $k$  retrieved samples.

Finally, we combine the two sources of information as:

$$z = \lambda \tilde{c} + (1 - \lambda) \tilde{s}, \quad (6)$$

where  $\lambda \in [0, 1]$  is a fixed hyperparameter controlling the relative contribution of each source of information. The fused representation  $z$ , which encodes (i) the query, (ii) the retrieved samples, and (iii) their relational information, is passed to the forecasting head to produce the prediction  $\hat{y}$ .

## 4 Experiments

### 4.1 Experimental Setup

**Pretraining datasets.** For pretraining, we use the Chronos pretraining dataset (Ansari et al., 2024), from which 50M data points are uniformly sampled, following the setup of prior work (Ning et al., 2025). A subset of 5M data points is further selected to construct a retrieval knowledge base. Both the pretraining dataset and the retrieval knowledge base are segmented using a fixed input window, resulting in 26M pretraining pairs and 2.8M retrieval pairs.

Table 3. Results of zero-shot forecasting across TSFMs. The proposed method outperforms existing TSFMs across diverse datasets, achieving up to a 4.8% MSE improvement over the best baseline. The 1<sup>st</sup> and 2<sup>nd</sup> results are indicated by **bold** and underline, respectively.

Methods	Cross-RAG (Ours)		Chronos-bolt (TMLR 2024)		MOMENT (ICML 2024)		TTM (NeurIPS 2024)		Moirai (ICML 2024)		TimesFM (ICML 2024)		Chronos (TMLR 2024)		Time-MoE (ICLR 2025)	
	MSE	MAE	MSE	MAE	MSE	MAE	MSE	MAE	MSE	MAE	MSE	MAE	MSE	MAE	MSE	MAE
ETTh1	<b>0.341</b>	<u>0.367</u>	<u>0.362</u>	<b>0.365</b>	0.392	0.411	0.362	0.371	0.369	0.384	0.425	0.383	0.422	0.381	0.362	<u>0.367</u>
ETTh2	<b>0.243</b>	<b>0.299</b>	<u>0.252</u>	<b>0.299</b>	0.274	0.333	0.253	0.303	0.255	0.305	0.289	0.323	0.266	0.314	0.252	0.322
ETTh1	<b>0.290</b>	<b>0.319</b>	<u>0.311</u>	<b>0.319</b>	0.351	0.383	0.315	<u>0.325</u>	0.540	0.432	0.332	0.333	0.394	0.370	0.321	0.334
ETTh2	<b>0.143</b>	<b>0.224</b>	<u>0.149</u>	<b>0.224</b>	0.170	0.258	0.151	<u>0.241</u>	0.196	0.269	0.170	0.255	0.166	0.252	0.157	0.254
Weather	<b>0.144</b>	<b>0.178</b>	<u>0.153</u>	<u>0.183</u>	0.180	0.238	0.154	0.189	0.171	0.191	—	—	0.190	0.211	0.149	0.184
Electricity	<b>0.112</b>	<b>0.200</b>	<u>0.113</u>	<b>0.200</b>	0.197	0.303	0.172	0.264	0.183	0.281	—	—	0.146	<u>0.224</u>	0.114	0.203
Exchange	<b>0.064</b>	<u>0.175</u>	0.067	0.178	0.098	0.206	<u>0.066</u>	<b>0.173</b>	<u>0.066</u>	0.172	0.070	0.180	0.083	0.188	0.085	0.206
Average	<b>0.191</b>	<b>0.252</b>	<u>0.201</u>	<u>0.253</u>	0.237	0.304	0.210	0.267	0.254	0.291	—	—	0.238	0.277	0.206	0.267

Table 4. Results of zero-shot forecasting across TS RAG methods. The proposed method outperforms existing RAG methods.

Method	ETTh1	ETTh2	ETTh1	ETTh2	Weather	Electricity	Exchange	Average
RAF (arXiv 2025)	0.366	0.252	0.306	0.148	0.178	0.119	<b>0.063</b>	0.205
TS-RAG (NeurIPS 2025)	<u>0.357</u>	<u>0.246</u>	<u>0.298</u>	<u>0.147</u>	<u>0.151</u>	<b>0.112</b>	0.071	<u>0.197</u>
Cross-RAG (Ours)	<b>0.341</b>	<b>0.243</b>	<b>0.290</b>	<b>0.143</b>	<b>0.144</b>	<b>0.112</b>	<u>0.064</u>	<b>0.191</b>

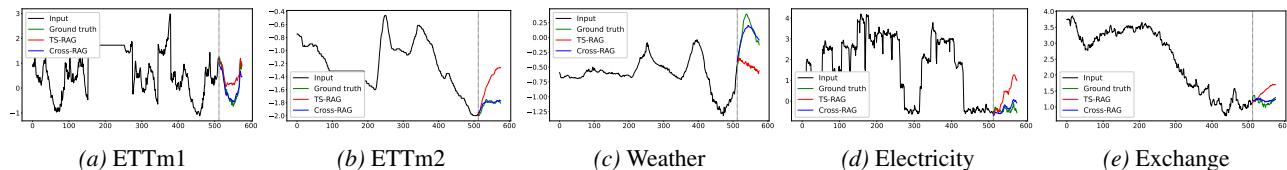


Figure 5. Visualization of zero-shot forecasting results (Cross-RAG vs. TS-RAG).

**Evaluation datasets.** Zero-shot evaluation is conducted on widely used time series benchmarks spanning diverse domains, four ETT datasets (ETTh1, ETTh2, ETTm1, ETTm2) (Zhou et al., 2021), Weather, Electricity, and Exchange (Wu et al., 2021). We maintain chronological order when separating the training, validation, and test sets, with split ratios of 6:2:2 for the ETT datasets and 7:1:2 for the remaining datasets. Details of datasets are provided in Appendix A.1.

**Baseline methods.** We compare our method with several TSFMs, including Chronos, Chronos-Bolt (Ansari et al., 2024), MOMENT (Goswami et al., 2024), TTM (Ekambaram et al., 2024), Moirai (Woo et al., 2024), TimesFM (Das et al., 2024), and Time-MoE (Shi et al., 2025). Details of baselines are provided in Appendix B.

**Experimental settings.** To remain consistent with standard settings, we fix the input length and forecasting horizon to 512 and 64, respectively, for both pretraining and evaluation, and use Chronos-Bolt as the TSFM backbone. For the evaluation metrics, we use mean squared error (MSE) and mean absolute error (MAE), and set  $k = 15$  and  $\lambda = 0.7$ . Note that we use  $k = 5$  for TS-RAG, which yields the best performance among values in  $[1, 15]$ . Details of experimental settings are reported in Appendix A.2

## 4.2 Zero-shot Forecasting

To validate the effectiveness of Cross-RAG, we evaluate it from two perspectives under zero-shot forecasting settings:

- (1) Comparison with TSFMs
- (2) Comparison with RAG methods

The baseline results are obtained both by reproducing experiments using the official implementations and by taking the reported results from the original paper (Ning et al., 2025).

**Comparison with TSFMs.** We compare our method with various TSFMs under the zero-shot forecasting setting. All models are evaluated without any task-specific fine-tuning, following the standard zero-shot protocol. Table 3 presents the results, demonstrating the effectiveness of our method in incorporating retrieval information for zero-shot forecasting and showing consistent improvements over TSFMs that rely solely on pretrained representations.

**Comparison with RAG methods.** We compare our method with RAG-based forecasting approaches under the same zero-shot forecasting setting. Table 4 shows the results, highlighting the effect of selectively attending to query-relevant retrieved samples. Additionally, Figure 5 visualizes the zero-shot forecasting results, showing that Cross-RAG follows the ground truth more closely than TS-RAG. Additional visualizations are provided in Section H.

Table 5. **Ablation on fusion components.**  $Q$  denotes the *skip-connection* from the **query** representation,  $R$  denotes *retrieval self-attention* that summarizes **retrieved samples**, and  $Q \leftrightarrow R$  denotes **query–retrieval cross-attention** between the query and retrieved samples.

$Q$	$R$	$Q \leftrightarrow R$	ETTh1	ETTh2	ETTm1	ETTm2	Weather	Electricity	Exchange	Average
✓			0.423	0.321	0.359	0.204	0.195	0.184	0.172	0.265
✓	✓		0.361	0.249	0.308	0.148	0.151	0.113	0.067	0.200
✓		✓	0.360	0.246	0.300	0.148	0.147	0.113	<b>0.066</b>	0.197
✓	✓	✓	<b>0.341</b>	<b>0.243</b>	<b>0.290</b>	<b>0.143</b>	<b>0.144</b>	<b>0.112</b>	<b>0.064</b>	<b>0.191</b>

Table 6. (R1) Performance (MSE/Rank) under various  $k$ s.

$k$	2	4	6	8	10	12	14
TS-RAG	.1975	.2011	.1968	.1975	.1967	.1974	.2013
Cross-RAG	<b>.1944</b>	<b>.1938</b>	<b>.1936</b>	<b>.1934</b>	<b>.1933</b>	<b>.1930</b>	<b>.1927</b>

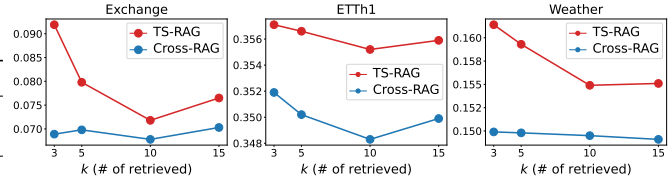
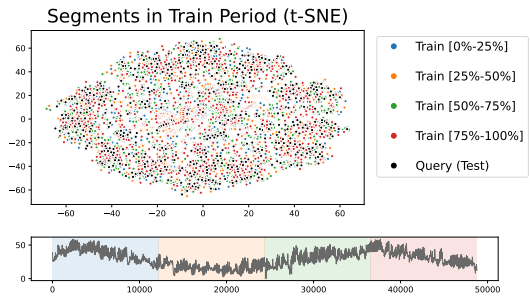


Figure 6. (R2) Performance under random retrieval.

Train period (%) ( $t = 0$ ← $t = T_{\text{train}}$ )				Methods	
Q1	Q2	Q3	Q4	TS-RAG	Cross-RAG
✓	✓	✓	✓	.1470	<b>.1435</b>
✗	✓	✓	✓	.1485	<b>.1463</b>
✗	✗	✓	✓	.1486	<b>.1458</b>
✗	✗	✗	✓	.1489	<b>.1467</b>

(a) (R3) Performance of ETTm2.



(b) (R3) Visualization of TS segments of ETTm2.

Figure 7. (R3) Performance under smaller knowledge base.

### 4.3 Ablation Studies

We conduct ablation studies to evaluate the contributions of Cross-RAG’s components: query skip-connection ( $Q$ ), retrieval self-attention ( $R$ ), and query–retrieval cross-attention ( $Q \leftrightarrow R$ ). Table 5 shows the results, demonstrating that using only the query representation ( $Q$ ) yields limited performance, while adding either retrieval self-attention ( $R$ ) or query–retrieval cross-attention ( $Q \leftrightarrow R$ ) consistently improves results. Combining all three components achieves the best performance across all datasets, highlighting the importance of jointly modeling the query, retrieved samples, and their input-level interactions. Additional ablation combinations are reported in Section D.

## 5 Analysis

### 5.1 Various Retrieval Scenarios

To validate the effectiveness of our method under various retrieval scenarios, we evaluate it across four settings:

- (R1) Retrieval with **various numbers of samples** ( $k$ )
- (R2) Retrieval of **random samples**
- (R3) Retrieval using a **smaller knowledge base**
- (R4) Retrieval from a **different dataset**

**(R1) Retrieval with various  $k$ s.** Table 6 and Figure 2a show the average MSE over seven datasets for various numbers of retrieved samples ( $k$ ). Unlike prior work (Ning et al., 2025), Cross-RAG consistently improves as  $k$  increases. These results indicate that simply increasing the number of retrieved samples does not improve performance unless relevance is considered, and that Cross-RAG effectively leverages additional samples by focusing on relevant ones. Full results for all datasets are reported in Section E.

**(R2) Retrieval of random samples.** To evaluate Cross-RAG’s ability to selectively attend to relevant retrieved samples, we conduct an experiment using *random* samples from the knowledge base, rather than selecting them based on similarity. Figure 6 presents the MSE over three datasets, showing that Cross-RAG consistently outperforms the SoTA method (Ning et al., 2025) for all values of  $k$ .

**(R3) Retrieval using a smaller knowledge base.** To evaluate the robustness of Cross-RAG under limited knowledge, we construct knowledge bases using *different fractions of the training dataset* using ETTm2, as shown in Figure 7b. Table 7a demonstrates that Cross-RAG consistently outperforms TS-RAG by effectively leveraging the available information even when the knowledge base is small.

Table 7. (R4) Retrieval from a different dataset.

KB → Target (KB: Knowledge Base)		Target			
		ETTh1	ETTh2	ETTh1	ETTh2
KB	ETTh1	<b>0.341</b>	<u>0.246</u>	0.325	0.149
	ETTh2	<u>0.351</u>	<b>0.243</b>	0.318	0.148
	ETTh1	0.370	0.250	<b>0.290</b>	<u>0.146</u>
	ETTh2	0.363	0.252	<u>0.304</u>	<b>0.143</b>
w/o Cross-RAG		0.362	0.252	0.311	0.149

Table 8. Average MSE across various input windows ( $T$ ) and forecast horizons ( $L$ ). Cross-attention-based retrieval in Cross-RAG leads to more consistent improvements compared with self-attention-based TS-RAG across seven different datasets.

(1) Input window ( $T$ )		with $L = 512$			
$T$	64	128	256	512	
TS-RAG	0.463	0.376	0.217	0.197	
Cross-RAG	<b>0.258</b>	<b>0.246</b>	<b>0.196</b>	<b>0.191</b>	
+ Imp. (%)	<b>+44.3%</b>	<b>+34.6%</b>	<b>+9.7%</b>	<b>+3.0%</b>	
(2) Forecast horizon ( $L$ )		with $T = 64$			
$L$	24	36	48	64	
TS-RAG	0.140	0.164	0.181	0.197	
Cross-RAG	<b>0.138</b>	<b>0.163</b>	<b>0.178</b>	<b>0.191</b>	
+ Imp. (%)	<b>+1.4%</b>	<b>+0.6%</b>	<b>+1.7%</b>	<b>+3.0%</b>	

Furthermore, we attribute this to the high redundancy of similar segments in historical data, as illustrated in Figure 7b. The figure shows that as recent segments cover a large portion of the relevant patterns, even a reduced knowledge base provides sufficient context for accurate retrieval, allowing Cross-RAG to maintain strong performance.

**(R4) Retrieval from a different dataset.** We further evaluate Cross-RAG in a setting where *no knowledge base is available from the target dataset* by constructing the knowledge base from *different* datasets. Specifically, we treat one of the four ETT datasets as the target and use the remaining three as the knowledge base. Table 7 reports the results, where Cross-RAG consistently outperforms the strong baseline (Chronos-Bolt) in most cases. In addition, stronger performance is observed when the knowledge base comes from the same or a similar domain (e.g., ETT hourly or ETT minutely), indicating more effective information transfer across aligned datasets.

## 5.2 Other Analyses

**Performance across various  $T, L$ s.** Table 8 reports the average MSE across various input windows ( $T$ ) and forecast

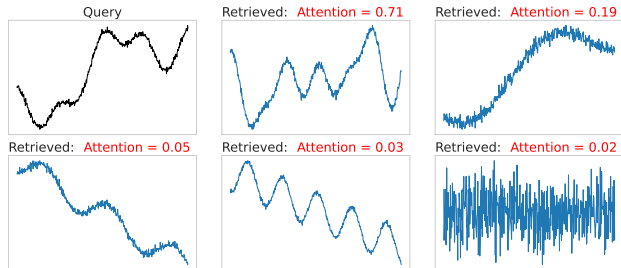


Figure 8. Attention of query and retrieved samples. The figure displays cross-attention weights between the input of *query* and *retrieved samples*, which assign high attention to relevant samples and low attention to irrelevant ones.

Table 9. Robustness to similarity metrics. Performance remains stable across different similarity metrics, indicating that the method can be applied directly in the data space without requiring a separate retrieval encoder.

	Data space			Latent space
	Cosine	Euclidean	Correlation	
ETTh1	0.341	0.343	0.348	0.347
ETTh2	0.243	0.248	0.245	0.244
ETTh1	0.290	0.294	0.297	0.294
ETTh2	0.143	0.143	0.144	0.144
Weather	0.144	0.146	0.146	0.145
Electricity	0.112	0.114	0.115	0.114
Exchange	0.064	0.067	0.069	0.067
Average	<b>0.191</b>	<u>0.193</u>	0.194	<u>0.193</u>

horizons ( $L$ ). We fix  $L = 64$  when varying the input window size ( $T$ ), and fix  $T = 512$  when varying the forecast horizon ( $L$ ). The proposed method consistently outperforms TS-RAG across all settings, with improvements pronounced for smaller input windows and longer forecast horizons.

**Attention weights across retrieved samples.** To examine how our proposed method attends to each retrieved sample for a given query, we construct a toy dataset and manually compose the retrieved set to include both relevant and irrelevant samples for each query. Figure 8 visualizes the results along with the (cross-) attention weights, showing that samples similar to the query receive higher weights, while irrelevant or noisy samples receive lower weights. More examples are visualized in Section G.

**Robustness to similarity metrics.** To examine the robustness to the choice of similarity metric used for retrieval, we conduct experiments under various similarity metrics across seven datasets. Specifically, we consider cosine similarity, Euclidean distance, correlation, and a latent-space metric (Euclidean). Table 9 reports the results, demonstrating that the performance remains stable across similarity metrics, suggesting that retrieval in the data space can be conducted without introducing an additional retrieval encoder.

Table 10. **Robustness to  $\lambda$** . Performance is stable across  $\lambda$ , and the fixed gating mechanism outperforms the learnable version.

$\lambda$	Learnable	Fixed				
		0.4	0.5	0.6	0.7	0.8
Avg. MSE	0.196	0.196	0.194	0.193	<b>0.191</b>	0.194

Table 11. **Efficiency analysis 1 - Retrieval**. The table compares retrieval in the latent space (w/ embedding) and the data space (w/o embedding) on ETTh1, showing that retrieval in the data space is substantially faster. More results are discussed in Section F.

Space	Procedures	Time (sec)
Latent ( $Z$ )	1) Embedding	381.6
	2) Search (FAISS)	2.1
	Total	383.7
Data ( $X$ )	1) Embedding	—
	2) Search (FAISS)	1.1
	Total	1.1
Speed-up ( $Z \rightarrow X$ )		<b>339.5<math>\times</math></b>

**Robustness to  $\lambda$** . To evaluate the robustness to  $\lambda$ , which controls the fusion of retrieved samples and the relational information between the query and these samples, we perform a sensitivity analysis across different  $\lambda$  values. We also test a learnable version of this gating mechanism, where two types of representations are concatenated and passed through an MLP followed by a sigmoid function. Table 10 reports the results, demonstrating that the performance is stable across  $\lambda$  and that the fixed gating mechanism outperforms the learnable version.

### 5.3 Efficiency Analyses

**Efficiency analysis 1 - Retrieval**. Table 11 compares retrieval in the data space and latent space using ETTh1. The results show that data-space retrieval is significantly faster, achieving a 339.5 $\times$  speed-up over latent-space retrieval, as it does not require any embedding computation. Search with FAISS corresponds to the offline construction of the retrieval index, where similar historical TS across all time-stamps and variables are precomputed and stored. During training and inference, only the stored index is accessed, without performing FAISS search repeatedly. Results for all datasets are discussed in Section F.

**Efficiency analysis 2 - Inference**. Table 12 compares inference efficiency on ETTh1 under different combinations of Cross-RAG components in terms of 1) inference time per instance (ms, averaged across 1000 runs) and 2) FLOPs. The inference cost remains nearly unchanged when incorporating the proposed components, demonstrating minimal computational overhead.

Table 12. **Efficiency analysis 2 - Inference**. Cross-RAG incurs negligible inference overhead in 1) inference time and 2) FLOPs.

$Q$	$R$	$Q \leftrightarrow R$	Inference time (ms)	FLOPs
✓			8.90	751.3M
✓	✓		9.69	755.5M
✓		✓	9.68	751.8M
✓	✓	✓	9.73	756.5M
TS-RAG			9.91	754.2M

Table 13. **Efficiency analysis 3 - Parameters**. Only the proposed attention modules and projectors are trainable, accounting for approximately 4% of the total parameters, while the remaining 96% (patch embedding, backbone) are frozen.

Components of Cross-RAG		# Params	Params (%)	
Patch Embedding	Input	2.5M	1.2%	
	Output	4.6M	2.1%	
Backbone	Encoder	85M	39.7%	
	Decoder	113M	52.9%	
+ Proposed	Attention	Self	3.5M	1.6%
		Cross	3.5M	1.6%
	Projector	Input	1.0M	0.5%
		Output	0.6M	0.3%

**Efficiency analysis 3 - Parameters**. As shown in Table 13, the proposed modules (e.g., attention and projector) account for approximately 4% of the total parameters, with all other modules frozen, ensuring high parameter efficiency. These learnable parameters are pretrained *only on the pretraining datasets* and remain fixed across all target datasets, consistent with the zero-shot setting.

## 6 Conclusion

In this work, we introduce Cross-RAG, a zero-shot retrieval-augmented framework for TS forecasting that selectively attends to query-relevant samples and models their input-level interactions via cross-attention. Our results show consistent improvements across diverse zero-shot scenarios and demonstrate effective selective retrieval with high efficiency, while remaining robust to variations in retrieval settings, distance metrics, and the choice of top- $k$ .

**Limitation and future works**. While Cross-RAG relies on input-level relationships for selective retrieval, it does not exploit auxiliary information, such as metadata. Future work includes adaptive retrieval and interaction mechanisms that incorporate this information across datasets.

## Impact Statement

This paper improves time series forecasting by incorporating retrieval-augmented generation into time series foundation models. The impact extends to domains where reliable forecasts are essential, including finance and healthcare, where improved predictions support informed decision-making and efficient resource allocation. We do not identify direct ethical concerns associated with this work. Overall, this study facilitates broader adoption of foundation models for complex time series analysis.

## References

- Ansari, A. F., Stella, L., Turkmen, C., Zhang, X., Mercado, P., Shen, H., Shchur, O., Rangapuram, S. S., Arango, S. P., Kapoor, S., et al. Chronos: Learning the language of time series. *arXiv preprint arXiv:2403.07815*, 2024.
- Chang, C., Peng, W.-C., and Chen, T.-F. Llm4ts: Two-stage fine-tuning for time-series forecasting with pre-trained llms. *CoRR*, 2023.
- Chen, S.-A., Li, C.-L., Yoder, N., Arik, S. O., and Pfister, T. Tsmixer: An all-mlp architecture for time series forecasting. *TMLR*, 2023.
- Cirstea, R.-G., Yang, B., Guo, C., Kieu, T., and Pan, S. Towards spatio-temporal aware traffic time series forecasting. In *2022 IEEE 38th International Conference on Data Engineering (ICDE)*, pp. 2900–2913. IEEE, 2022.
- Das, A., Kong, W., Sen, R., and Zhou, Y. A decoder-only foundation model for time-series forecasting. *ICML*, 2024.
- Ekambaram, V., Jati, A., Dayama, P., Mukherjee, S., Nguyen, N., Gifford, W. M., Reddy, C., and Kalagnanam, J. Tiny time mixers (tms): Fast pre-trained models for enhanced zero/few-shot forecasting of multivariate time series. *NeurIPS*, 37:74147–74181, 2024.
- Garza, A., Challu, C., and Mergenthaler-Canseco, M. Timegpt-1. *arXiv preprint arXiv:2310.03589*, 2023.
- Goswami, M., Szafer, K., Choudhry, A., Cai, Y., Li, S., and Dubrawski, A. Moment: A family of open time-series foundation models. In *ICML*, 2024.
- Han, S., Lee, S., Cha, M., Arik, S. O., and Yoon, J. Retrieval augmented time series forecasting. *ICML*, 2025.
- Huang, Q., Shen, L., Zhang, R., Ding, S., Wang, B., Zhou, Z., and Wang, Y. Crossggn: Confronting noisy multivariate time series via cross interaction refinement. *Advances in Neural Information Processing Systems*, 36: 46885–46902, 2023.
- Jiang, Y., Chen, Y., Li, X., Chao, Q., Liu, S., and Cong, G. Fstllm: Spatio-temporal llm for few shot time series forecasting. In *ICML*, 2025.
- Jing, B., Zhang, S., Zhu, Y., Peng, B., Guan, K., Margenot, A., and Tong, H. Retrieval based time series forecasting. *CIKM*, 2022.
- Lewis, P., Perez, E., Piktus, A., Petroni, F., Karpukhin, V., Goyal, N., Küttler, H., Lewis, M., Yih, W.-t., Rocktäschel, T., et al. Retrieval-augmented generation for knowledge-intensive nlp tasks. *NeurIPS*, 33:9459–9474, 2020.
- Liu, J., Yang, L., Li, H., and Hong, S. Retrieval-augmented diffusion models for time series forecasting. *NeurIPS*, 37: 2766–2786, 2024a.
- Liu, Y., Hu, T., Zhang, H., Wu, H., Wang, S., Ma, L., and Long, M. itransformer: Inverted transformers are effective for time series forecasting. In *ICLR*, 2024b.
- Liu, Y., Zhang, H., Li, C., Huang, X., Wang, J., and Long, M. Timer: Generative pre-trained transformers are large time series models. In *ICML*, 2024c.
- Liu, Y., Qin, G., Shi, Z., Chen, Z., Yang, C., Huang, X., Wang, J., and Long, M. Sundial: A family of highly capable time series foundation models. *ICML*, 2025.
- Luo, D. and Wang, X. Moderntcn: A modern pure convolution structure for general time series analysis. In *The twelfth international conference on learning representations*, pp. 1–43, 2024.
- Ning, K., Pan, Z., Liu, Y., Jiang, Y., Zhang, J. Y., Rasul, K., Schneider, A., Ma, L., Nevmyvaka, Y., and Song, D. Ts-rag: Retrieval-augmented generation based time series foundation models are stronger zero-shot forecaster. *NeurIPS*, 2025.
- Niu, W., Xie, Z., Sun, Y., He, W., Xu, M., and Hao, C. Lang-time: A language-guided unified model for time series forecasting with proximal policy optimization. *ICML*, 2025.
- Raffel, C., Shazeer, N., Roberts, A., Lee, K., Narang, S., Matena, M., Zhou, Y., Li, W., and Liu, P. J. Exploring the limits of transfer learning with a unified text-to-text transformer. *Journal of machine learning research*, 21 (140):1–67, 2020.
- Rasul, K., Ashok, A., Williams, A. R., Khorasani, A., Adamopoulos, G., Bhagwatkar, R., Biloš, M., Ghonia, H., Hassen, N., Schneider, A., et al. Lag-llama: Towards foundation models for time series forecasting. In *RO-FoMo: Robustness of Few-shot and Zero-shot Learning in Large Foundation Models*, 2023.

- Rezaei, H., Faaljoui, H., and Mansourfar, G. Stock price prediction using deep learning and frequency decomposition. *Expert Systems with Applications*, 169:114332, 2021.
- Shi, X., Wang, S., Nie, Y., Li, D., Ye, Z., Wen, Q., and Jin, M. Time-moe: Billion-scale time series foundation models with mixture of experts. *ICLR*, 2025.
- Sun, C., Li, H., Li, Y., and Hong, S. Test: Text prototype aligned embedding to activate llm’s ability for time series. *ICLR*, 2024.
- Tan, M., Merrill, M., Gupta, V., Althoff, T., and Hartvigsen, T. Are language models actually useful for time series forecasting? *NeurIPS*, 37:60162–60191, 2024.
- Tire, K., Taga, E. O., Ildiz, M. E., and Oymak, S. Retrieval augmented time series forecasting. *arXiv preprint arXiv:2411.08249*, 2024.
- Woo, G., Liu, C., Kumar, A., Xiong, C., Savarese, S., and Sahoo, D. Unified training of universal time series forecasting transformers. In *ICML*, 2024.
- Wu, H., Xu, J., Wang, J., and Long, M. Autoformer: Decomposition transformers with auto-correlation for long-term series forecasting. In *NeurIPS*, 2021.
- Xu, Z., Liu, X., Xu, Q., Su, X., Guo, X., and Wang, Y. Time series forecasting with attention-augmented recurrent networks: A financial market application. In *Proceedings of the 2025 2nd International Conference on Computer and Multimedia Technology*, pp. 155–159, 2025.
- Xue, H. and Salim, F. D. Promptcast: A new prompt-based learning paradigm for time series forecasting. *TKDE*, 36(11):6851–6864, 2023.
- Yang, S., Wang, D., Zheng, H., and Jin, R. Timerag: Boosting llm time series forecasting via retrieval-augmented generation. In *ICASSP*, pp. 1–5. IEEE, 2025.
- Zhou, H., Zhang, S., Peng, J., Zhang, S., Li, J., Xiong, H., and Zhang, W. Informer: Beyond efficient transformer for long sequence time-series forecasting. In *AAAI*, 2021.
- Zhou, T., Niu, P., Sun, L., Jin, R., et al. One fits all: Power general time series analysis by pretrained lm. In *NeurIPS*, 2023.

## Appendix

### A Experimental Settings

#### A.1 Dataset Statistics

**Inference dataset for zero-shot forecasting.** We conduct experiments on seven datasets spanning diverse domains, with dataset statistics summarized in Table A.1, where  $C$  and  $T$  denote the number of channels and timesteps, respectively. The training split is used to construct the knowledge base, while the test split is used for zero-shot inference.

Table A.1. Statistics of inference dataset for zero-shot forecasting.

Dataset	$C$	$T$	$(N_{\text{train}}, N_{\text{val}}, N_{\text{test}})$
ETTh1 (Zhou et al., 2021)	7	17420	(8545, 2881, 2881)
ETTh2 (Zhou et al., 2021)	7	17420	(8545, 2881, 2881)
ETTm1 (Zhou et al., 2021)	7	69680	(34465, 11521, 11521)
ETTm2 (Zhou et al., 2021)	7	69680	(34465, 11521, 11521)
Exchange (Wu et al., 2021)	8	7588	(5120, 665, 1422)
Weather (Wu et al., 2021)	21	52696	(36792, 5271, 10540)
Electricity (Wu et al., 2021)	321	26304	(18317, 2633, 5261)

#### A.2 Experimental Details

We follow the experimental settings of TS-RAG (Ning et al., 2025), where the backbone TSFM remains frozen during pretraining, and only the parameters introduced by Cross-RAG, including attention modules and projectors, are updated. Chronos-Bolt (Ansari et al., 2024) serves as the backbone, and we adopt its original quantile regression loss. All experiments are conducted on a single NVIDIA L40-48G GPU. Details of training hyperparameters are summarized in Table A.2.

Table A.2. Details of training hyperparameters.

Optimizer	AdamW
Learning rate	$3 \times 10^{-4}$
Weight decay	0.01
Batch size	256
Training steps	10,000
Dropout rate	0.2
Retrieved sequences ( $k$ )	15

## B Baseline Methods

- **Chronos** (Ansari et al., 2024): A probabilistic TSFM that tokenizes quantized TS and processes them with a T5 backbone (Raffel et al., 2020).
- **Chronos-Bolt** (Ansari et al., 2024): A Chronos variant that supports patch-based modeling and generates multi-step quantile forecasts using decoder representations.
- **MOMENT** (Goswami et al., 2024): A zero-shot TSFM applies masked modeling by appending a masked forecast horizon to the lookback sequence.
- **TTM** (Ekambaram et al., 2024): A compact TSFM based on TSMixer (Chen et al., 2023) with adaptive patching and resolution-aware pretraining.
- **Moirai** (Woo et al., 2024): A Transformer encoder pretrained on LOTSA via horizon masking and reconstruction across target channels.
- **TimesFM** (Das et al., 2024): A decoder-style attention model pretrained on large-scale real and synthetic TS.
- **Time-MoE** (Shi et al., 2025): A decoder-only TSFM with a mixture-of-experts (MoE) architecture for autoregressive forecasting with long contexts.

## C Similarity Metrics

For the experiments, we use four different similarity metrics for retrieving similar samples:

- **Cosine similarity (data space)** measures the similarity between two TS based on the angle between their vectors in the data space, capturing pattern-level similarity while being invariant to scale.
- **Euclidean distance (data space)** computes the  $\ell_2$  distance between raw TS, directly reflecting point-wise magnitude differences.
- **Pearson correlation (data space)** quantifies the linear relationship between two TS, providing a normalized similarity measure invariant to mean and variance.
- **Euclidean distance (latent space)** measures the  $\ell_2$  distance between latent representations produced by an retrieval encoder, capturing similarity in the learned representation space.

For cosine similarity and Euclidean distance in the data space, each TS is first normalized to the  $[0, 1]$  range using min-max scaling before computing the similarity. As robustness is consistently observed with these similarity metrics, Dynamic Time Warping (DTW) is omitted due to its high computational complexity.

## D Ablation Studies

We conduct an ablation study to assess the effect of the query skip-connection ( $Q$ ), retrieval self-attention ( $R$ ), and query-retrieval cross-attention ( $Q \leftrightarrow R$ ). Table D.1 reports the full results, where combining all three components yields the best performance.

Table D.1. Full results of ablation on fusion components.  $Q$  denotes the skip-connection from the query representation,  $R$  denotes retrieval self-attention that summarizes retrieved samples.

$Q$	$R$	$Q \leftrightarrow R$	ETTh1	ETTh2	ETTm1	ETTm2	Weather	Electricity	Exchange	Average
✓			0.423	0.321	0.359	0.204	0.195	0.184	0.172	0.265
	✓		0.717	0.364	0.697	0.284	0.263	0.848	0.364	0.505
		✓	0.405	0.282	0.348	0.177	0.171	0.168	0.128	0.240
✓	✓		0.361	0.249	0.308	0.148	0.151	0.113	0.067	0.200
✓		✓	0.360	0.246	0.300	0.148	0.147	0.113	0.066	0.197
	✓	✓	0.393	0.279	0.329	0.171	0.164	0.164	0.115	0.231
✓	✓	✓	<b>0.341</b>	<b>0.243</b>	<b>0.290</b>	<b>0.143</b>	<b>0.144</b>	<b>0.112</b>	<b>0.064</b>	<b>0.191</b>

## E Various Number of Retrieved Sequences ( $k$ s)

To assess zero-shot forecasting performance under different numbers of retrieved samples ( $k$ ), we conduct an evaluation with varying values of  $k$ . Table E.1 reports the results, showing that the average performance across seven datasets improves as  $k$  increases.

Table E.1. Zero-shot forecasting performance (MSE) under various  $k$ s.

$k$	ETTh1	ETTh2	ETTm1	ETTm2	Weather	Electricity	Exchange	Average
1	0.3513	0.2457	0.2986	0.1441	0.1462	0.1158	0.0656	0.1953
2	0.3476	0.2464	0.2976	0.1435	0.1458	0.1145	0.0652	0.1944
3	0.3466	0.2467	0.2966	0.1433	0.1454	0.1143	0.0648	0.1940
4	0.3462	0.2466	0.2956	0.1434	0.1453	0.1141	0.0652	0.1938
5	0.3461	0.2468	0.2945	0.1435	0.1455	0.1141	0.0653	0.1937
6	0.3465	0.2474	0.2937	0.1432	0.1453	0.1139	0.0653	0.1936
7	0.3449	0.2484	0.2940	0.1437	0.1452	0.1143	0.0655	0.1937
8	0.3444	0.2469	0.2925	0.1436	0.1449	0.1139	0.0658	0.1934
9	0.3444	0.2469	0.2928	0.1436	0.1448	0.1139	0.0658	0.1932
10	0.3451	0.2467	0.2922	0.1425	0.1447	0.1142	0.0675	0.1933
11	0.3451	0.2465	0.2928	0.1436	0.1450	0.1139	0.0665	0.1933
12	0.3449	0.2462	0.2912	0.1434	0.1450	0.1141	0.0663	0.1930
13	0.3451	0.2462	0.2913	0.1432	0.1447	0.1140	0.0663	0.1930
14	0.3441	0.2451	0.2905	0.1438	0.1444	0.1139	0.0673	0.1927
15	0.3411	0.2427	0.2896	0.1435	0.1437	0.1123	0.0645	<b>0.1911</b>

## F Efficiency Analysis

Table F.1 compares retrieval in the data space and latent space using five different datasets. Since ETTh1 and ETTh2 share the same data size, as do ETTm1 and ETTm2, we report only one dataset from each pair. The results demonstrate that the retrieval in the data-space is significantly faster than in the latent space, data-space retrieval is significantly faster,

Table F.1. Efficiency analysis under five different datasets.

Space	Retrieval procedures	Dataset				
		ETTh1	ETTm1	Exchange	Weather	ECL
Latent space ( $Z$ )	1) Embedding	381.6	1547.4	196.7	3530.1	27514.5
	2) Search (FAISS)	2.1	19.4	0.7	37.1	253.5
	Total	383.7	1566.8	197.4	3587.2	27768.0
Data space ( $X$ )	1) Embedding	—	—	—	—	—
	2) Search (FAISS)	1.1	16.5	0.4	22.2	129.3
	Total	1.1	16.5	0.4	22.2	129.3

## G Visualization of Inputs of Query and Retrieved Samples

To analyze how Cross-RAG assigns attends to retrieved samples for a given query, we design a toy dataset containing both relevant and irrelevant retrieved sequences. Figure G.1 presents the resulting cross-attention weights, where retrieved samples that resemble the query receive higher weights, whereas unrelated or noisy samples are assigned lower weights.

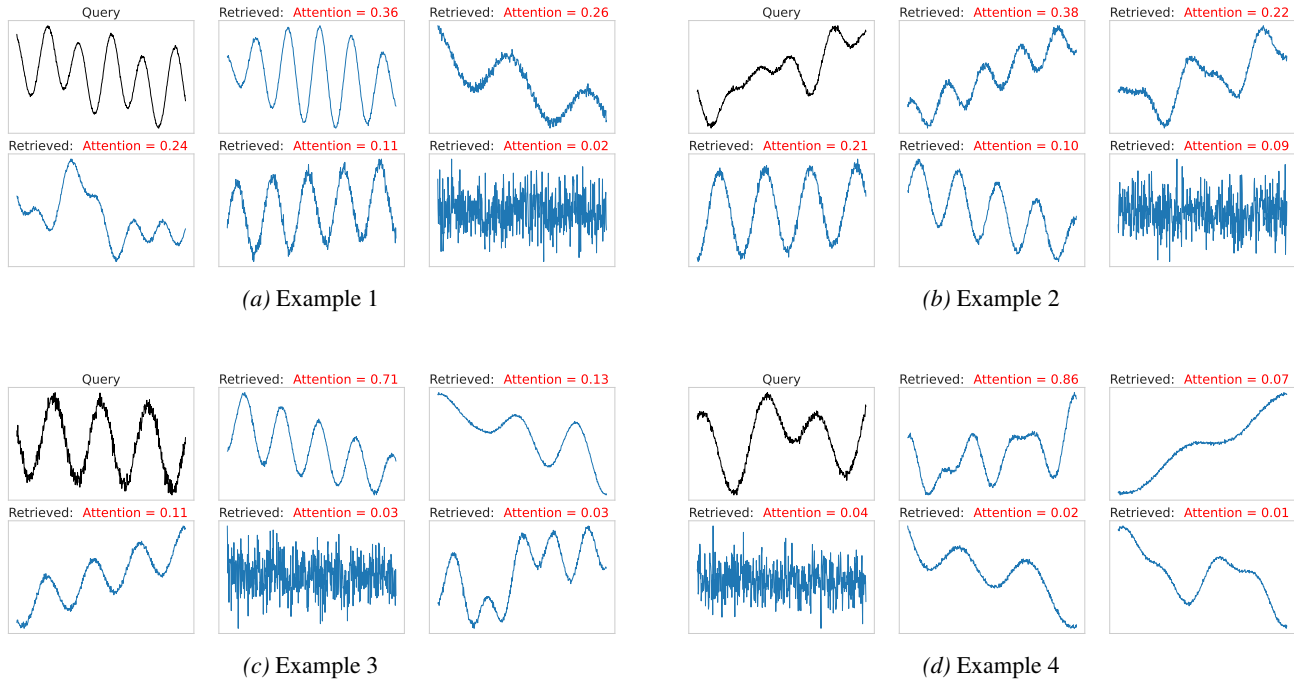


Figure G.1. Visualization of inputs of query and retrieved samples with toy datasets.

## H Visualization of Zero-shot Forecasting

We visualize the predicted results on six different datasets and compare them with TS-RAG(Ning et al., 2025).

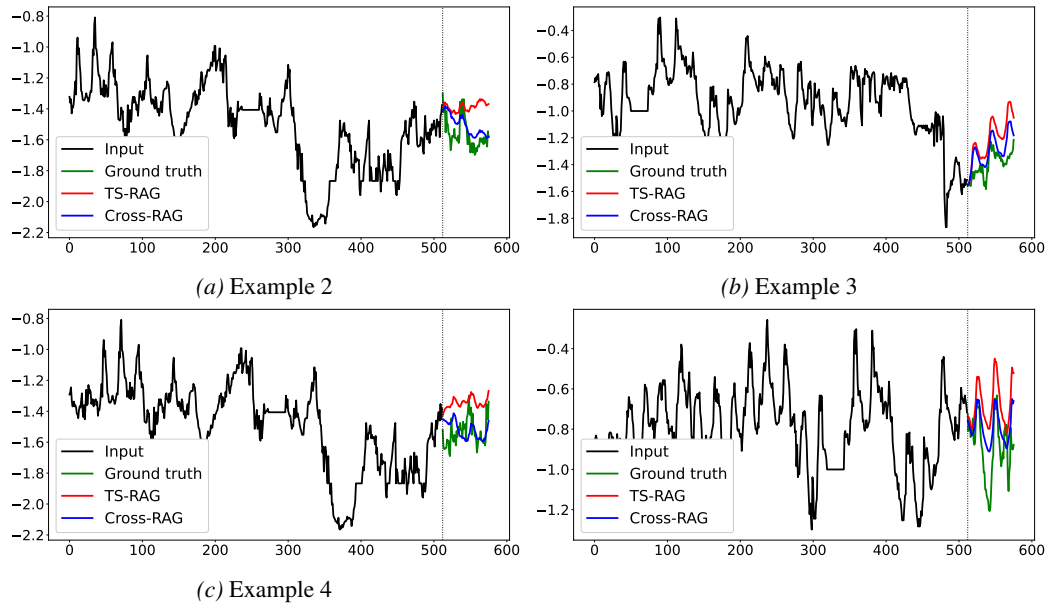


Figure H.1. Visualization of zero-shot forecasting on **ETTh1**.

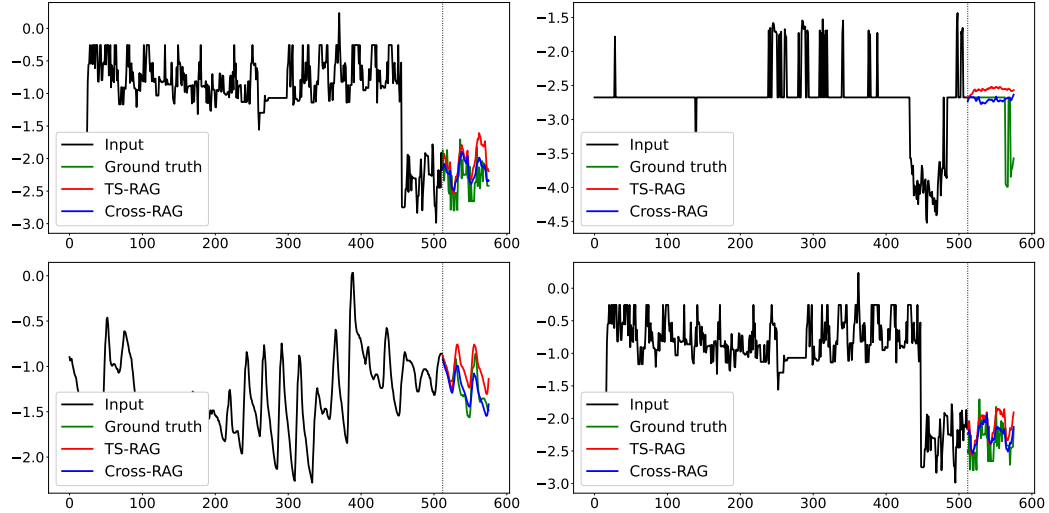


Figure H.2. Visualization of zero-shot forecasting on **ETTh2**.

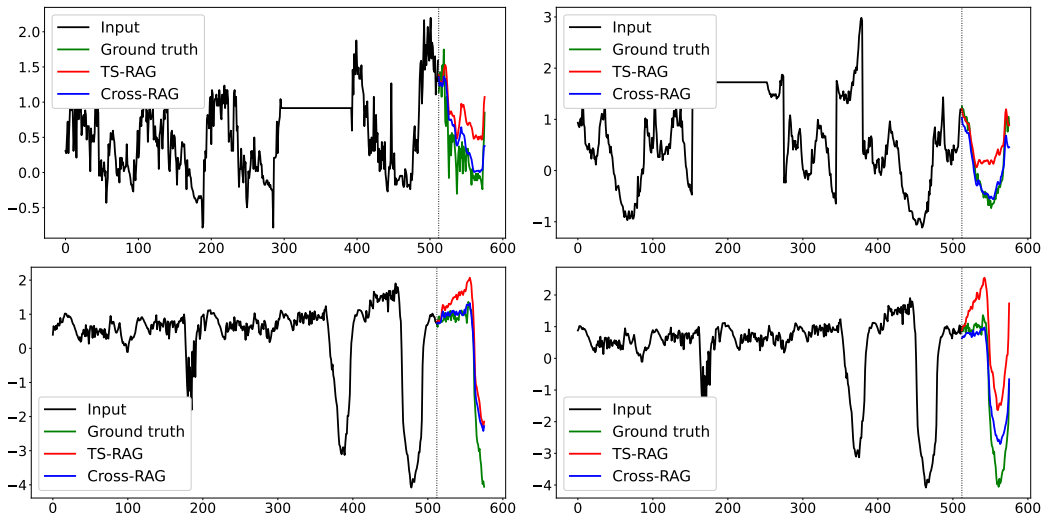


Figure H.3. Visualization of zero-shot forecasting on ETTm1.

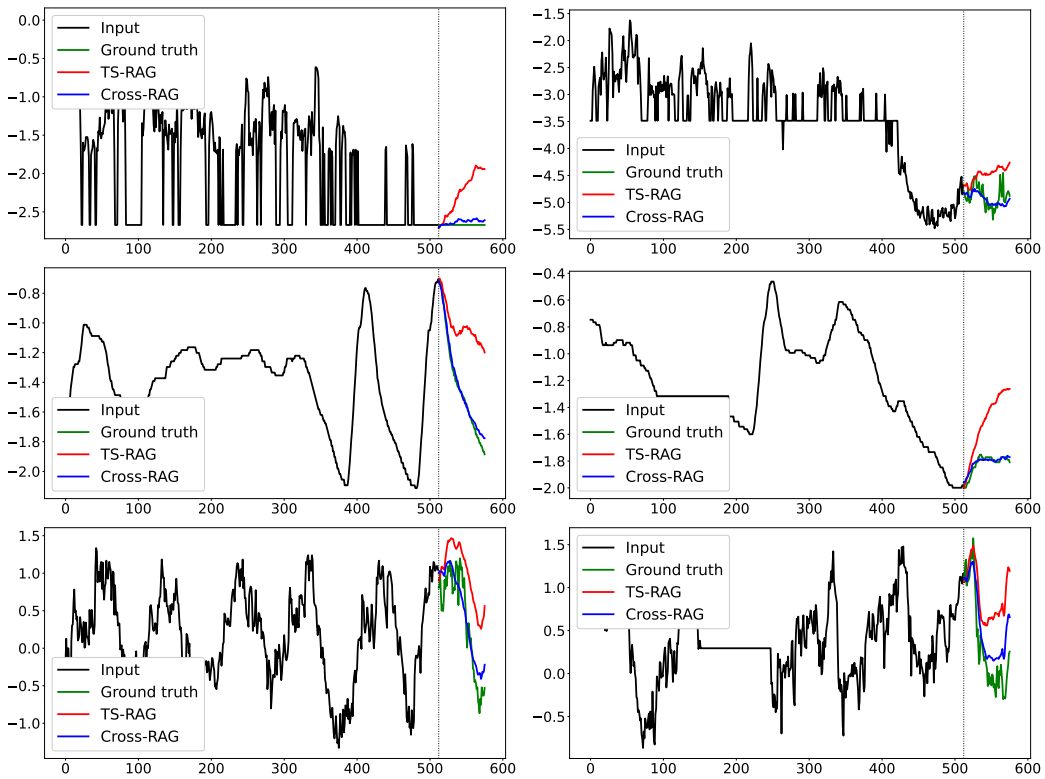


Figure H.4. Visualization of zero-shot forecasting on ETTm2.

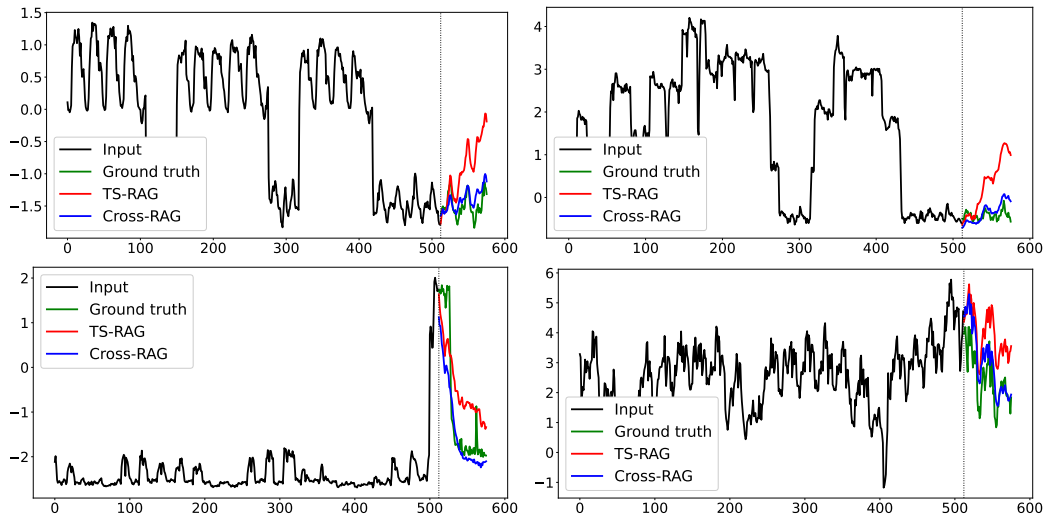


Figure H.5. Visualization of zero-shot forecasting on **Electricity**.

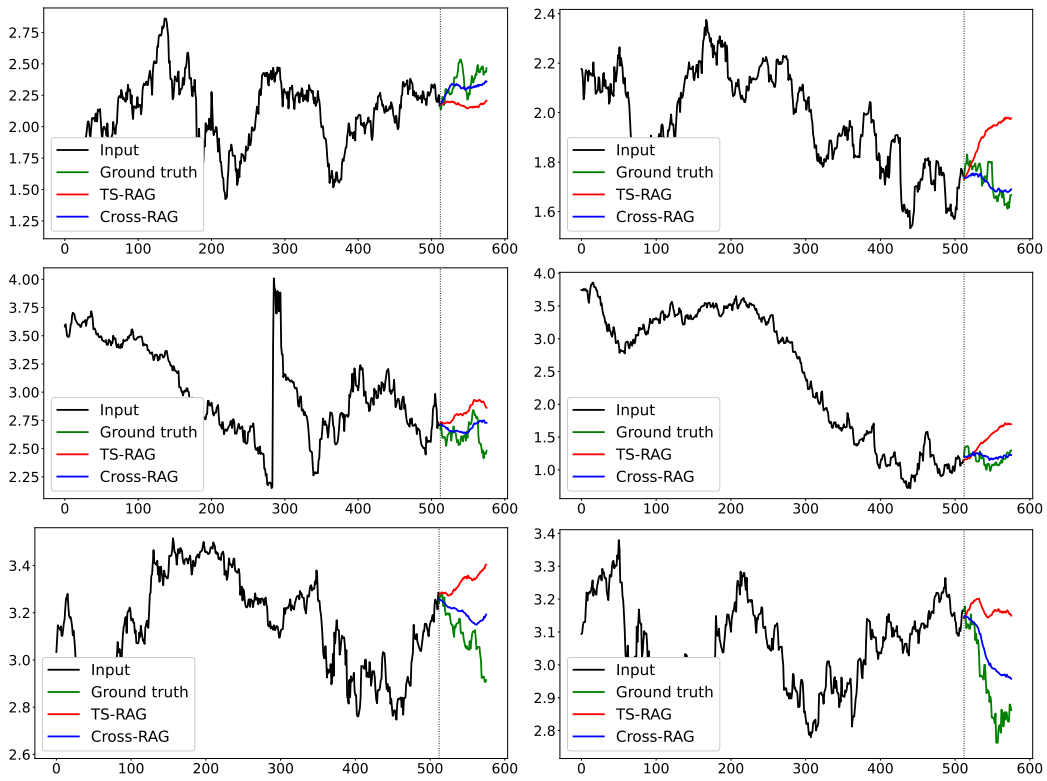


Figure H.6. Visualization of zero-shot forecasting on **Exchange**.

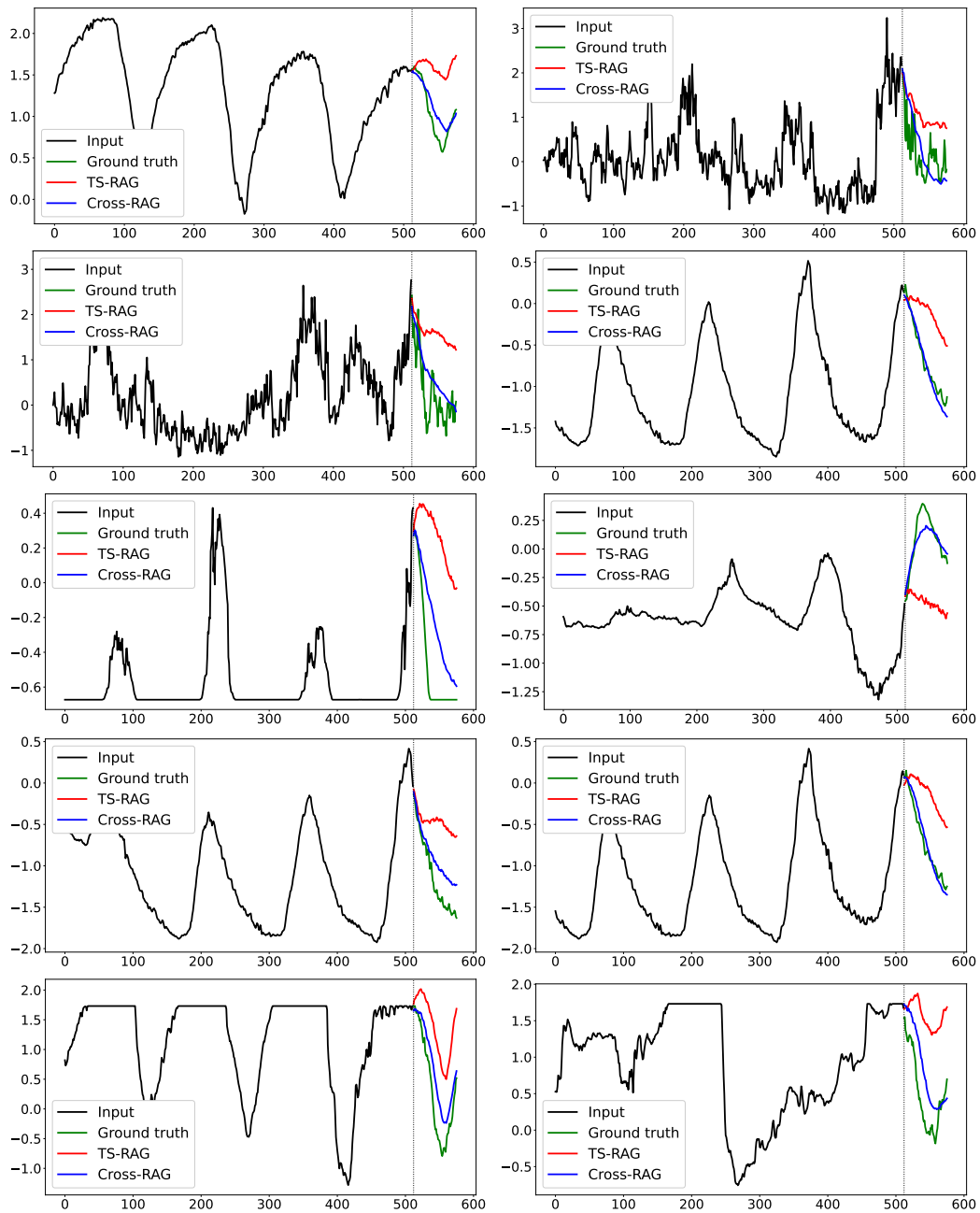


Figure H.7. Visualization of zero-shot forecasting on **Weather**.